

# Lateral Offset Estimation Based on Detection of Lane Markings

Gang Yi Jiang, Jong Wook Park, Byung Suk Song\*, Jae Wook Bae\*  
Tae Young Choi, Suk Kyo Hong

Division of Electronics Engineering, Ajou University, \*Institute of Advanced Engineering  
5 Wonchon-dong, Paldal-ku, Suwon-city, 442-749, KOREA

\*YoungIn P.O.Box 25, Kyonggi-Do, 449-020, KOREA

Tel: +82-331-219-2362, Fax: +82-331-212-9531

E-mail: imagepjw@madang.ajou.ac.kr

**Abstract:** In this paper, a new lateral offset estimation method, based on image processing techniques, is proposed for driver assistant system. A new description on lane markings in the image plane is presented, and its properties are discussed and used to detect lane markings. Multi-frame lane detection and analysis are adopted to improve the proposed lateral control method. An algorithm for obstacle detection is also developed. Experimental results show that the proposed method performs lateral control effectively.

## 1. Introduction

A numerous accidents are often caused due to driver inattention or driver impairment. To reduce the accidents, a driver assistant system is designed to warn the driver and to help him to keep the vehicle in path when the vehicle is about to depart the roadway [1]. Lateral control module, as a key part in driver assistant system, is used to detect and estimate the lateral distance of a vehicle [2].

In general, the approaches for lateral control are mainly classified into two ways, that is, using road boundaries (or lane markings) [3-5], based on neural networks [6], and using a target point in the field of view [7]. For the lateral control, the most crucial variables to be sensed are the position and orientation of the vehicle relative to road boundary. In addition to these parameters, sensing of road curvature is quite significant as it facilitates a smoother trajectory. Most of methods exploit the information of road boundaries or lane markings, in which lateral control depends on lane following and lane changing. Other methods use a target point in the field of view, where lateral control relies on obstacle detection. An alternative technique is based on the detection of light reflectors, which is often placed on the both sides of existing infrastructures [8].

This work focuses on the development of a vision-based system for lateral vehicle control with detecting and tracking lane marking. Lane markings in two-dimensional (2D) image plane are decomposed into two parts: the upper and lower, their properties are discussed and used to develop a new lane detection algorithm in Section 2. A binary rank order transform (BROT) [9] is used to detect obstacle. Analysis of lane structure is given in Section 3, and experimental results of lateral control are shown in Section 4.

## 2. New Method for Lane Detection

Fig. 1 shows a lane model in two-dimensional (2D) image plane. It is obvious that the lane markings close to

the lower half of the image have more pixels, while the lane markings in the upper half of image possess less pixels. In fact, each segment of lane markings in real world is artificially designed to be of the same length and width. Moreover, highways and expressways are usually designed to have small curvature. According to the discussions, lane markings are described as two parts: the lower lane markings (LLM) and the upper lane markings (ULM), in this paper.

The properties of LLM and ULM are described as follows

- (1) In 2D image plane, LLM are usually major parts of lane markings, and they are longer and larger than ULM due to the perspective effect.
- (2) In 3D real world, LLM are only minor parts of lane markings ahead of the vehicle, while ULM is the major part to be processed.
- (3) In 3D real world, LLM represents the tangent of lane, while ULM describes the curvature of lane.
- (4) The slopes of LLM are mainly relative to the lateral offset, but not with the lane curvature. LLM in 3D real world can be used to analyze the vehicle heading direction.
- (5) If the lane is approximately in the center of 2D image plane, the slope  $\rho_L$  of the left LLM is usually positive, whereas the slope  $\rho_R$  of the right LLM is negative.
- (6) In 2D image plane, two fitted-lines of LLM intersect at a point, which is an estimation of vanishing point and called as quasi-vanishing point (QVP). The distance between QVP and the intersection of the left and right ULM describes the degree of lane curvature. When lane goes straightly, the distance is near to zero. Conversely, if the distance is very large, it implies that the road curves largely. For road image sequences of expressways and highways, QVP varies without sudden changes if images are normally taken.

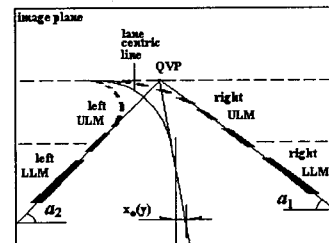


Fig. 1 Lane model in 2D image plane

Consider that ULM in input image are often not obvious so that they are not easy to be detected directly, we first extract LLM regions, and then detect ULM using the information on the detected LLM. An efficient approach to lane detection is proposed in Fig.2.

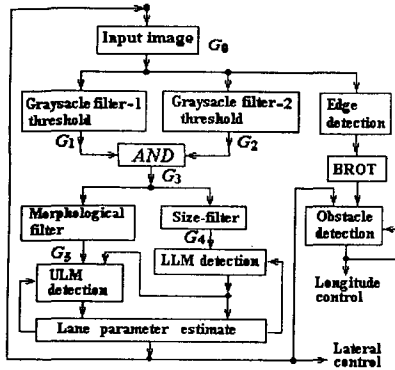


Fig. 2 New method for lane and obstacle detection

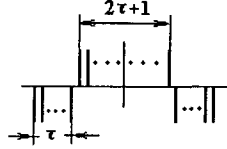


Fig. 3 Window of gray-scale filter-1

For a given road image  $G_0$ ,  $G_0 = \{g_0(u,v); 0 \leq u < N, 0 \leq v < M\}$ , it is processed by two gray-scale filters and threshold, and two binary images  $G_1$  and  $G_2$  are obtained. Gray-scale filter-1 is one-dimensional filter with a variable window in Fig. 3. Its window width  $(2\tau+1)$  varies with the vertical coordinate of the filtered pixel, and defined by

$$\begin{cases} \tau = \tau_0 & v < v_0 \\ \tau = \tau_0 + k_0(v - v_0) & v_0 \leq v \leq v_1 \\ \tau = \tau_1 & v > v_1 \end{cases} \quad (1)$$

where  $0 \leq v < M$ .  $\tau_0$ ,  $\tau_1$ ,  $v_0$ ,  $v_1$  and  $k_0$  are constants,  $\tau_0 > \tau_1$ ,  $k_0 < 0$ , which rely on camera parameters.

Gray-scale filter-2 is a mean filter with the window width of  $(2\tau+1)$ . A logic "AND" operation between  $G_1$  and  $G_2$  is performed to create an image  $G_3$ .  $G_3$  is simplified and smoothed by a size filter to obtain an image  $G_4$ , in which the LLM regions in the current lane are detected, exploiting the information on LLM in the previous input image. Furthermore, the equations of two fitted-lines of LLM are estimated and QVP is located.

$G_3$  is also filtered by morphological closing and simplified to produce an image  $G_5$ , in which the regions of ULM are searched by using the LLM regions of the current input image and ULM information of the previous input image. Then, lane state analysis is performed and lane state parameters are estimated accurately and stored. Lane tracking is used. The obtained parameters of lane detection are used for vehicle control or warning driver.

To improve the robustness and reliability of the lane detection algorithm, the lane structure in the previous input image is also used to improve and speed up the performances of LLM detection and ULM detection, as shown in Fig. 2. The use of the previous lane structure will produce well performance even though the lane markings in the current input image are probably hidden. The spatial and temporal continuity can also be exploited to recover the lost information, caused by shadows and obstructions from other vehicles.

Additionally, it is known that the lines, which lie parallel to 2D image plane in 3D scene, will not vanish

in the perspective image. In a 2D road image, vertical edges of a vehicle remain vertical and do not converge. The fact is helpful of detecting obstacles from 2D image plane. Based on edge information of obstacles in road image an obstacle detection approach is proposed in Fig.2. Edges in the regions of the current lane and neighboring lanes are detected, and BROT with vertical line structuring element is performed to smooth the vertical edges and remove the edges that do not belong to the vertical edges of vehicle. BROT of binary image  $X$  with structuring element  $B$ , denoted  $X \oplus B$ , is defined by

$$X \oplus B = \{a; \text{Card}(X \cap B_a) \geq G - (G-1)P\} \quad (2)$$

where  $p=0, 1/(G-1), 2/(G-1), \dots, 1$ .  $G = \text{Card}(B)$  is the cardinality of  $B$ .

Then, the resultant vertical edges are exploited to determine whether there is any obstacle or not.

Finally, the estimated lane structure parameters and detected obstacle are used to control the lateral and longitude distances of the vehicle.

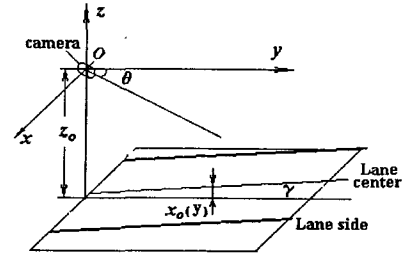


Fig. 4 Lane model in 3D real world

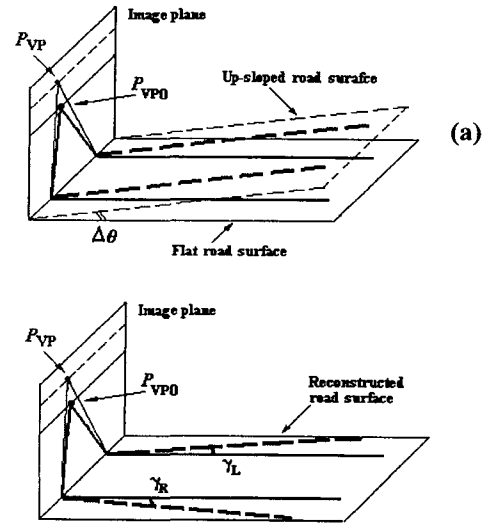


Fig. 5 (a) Perspective projection of lane markings, (b) 3D reconstruction of 2D image plane

### 3. Analysis of Lane Geometry

To obtain precise estimation of lateral offset, a geometric model in Fig.4 is adopted. In the figure,  $x_0$ ,  $z_0$ ,  $\gamma$  and  $\theta$  denote lateral offset of vehicle, camera height from the ground, vehicle deviation angle, and inclination camera angle, respectively. Consider that the perspective effect leads to image pixels having different meanings in the image plane, 3D reconstruction should be performed, so that the lateral offset and curvature of lane can be computed accurately in 3D real world. A point  $P(x,y,z)$  in

the real world  $\underline{W}$  is mapped into  $Q(u,v)$  in the image plane  $\underline{I}$  and represented by

$$u = \frac{fx}{y \cos \theta - z \sin \theta}, \quad v = \frac{f(z \cos \theta + y \sin \theta)}{y \cos \theta - z \sin \theta} \quad (3)$$

where  $f$  is the focus distance of the camera. Similarly, a point  $Q(u,v)$  in  $\underline{I}$  is mapped into  $P(x,y,z)$  in  $\underline{W}$  and expressed by

$$x = \frac{uz_0}{v \cos \theta - f \sin \theta}, \quad y = \frac{z_0(f \cos \theta + v \sin \theta)}{v \cos \theta - f \sin \theta},$$

and  $z = z_0,$  (4)

Perspective projection of any set of parallel lines in 3D world, but not parallel to 2D image plane, converges to a vanishing point (or QVP). The location of a QVP determined by LLM indicates the direction of the road. Fig. 5(a) shows the perspective projection of flat and up-sloped road surfaces, where  $P_{VP0}$  and  $P_{VP}$  are the corresponding vanishing points, respectively. There is an angle  $\Delta\theta$  between the flat and up-sloped road surfaces, which results in that the vanishing point of the lane markings on the up-sloped road surface moves upwards. Fig. 5(b) shows a 3D reconstruction of the 2D image plane in Fig. 5(a), in which the solid and dash lines express the lane markings, corresponding to the flat and the up-sloped road surfaces, respectively. There are two angles,  $\gamma_L$  and  $\gamma_R$ , between the reconstructed lane markings, which can be used to estimate the slope  $\Delta\theta$ , so that accurate reconstruction is obtained to estimate the parameters of lane structure. For a down-slope road surface, the practical vanishing point moves downwards.

#### 4. Experimental Results

Quantities of experiments have been implemented to test the new method with our experimental system. Fig. 6 shows one of performances. Fig. 6(a) is an input image  $G_0$ . After pre-processing, two binary images,  $G_1$  and  $G_2$ , are obtained and used to produce  $G_3$  in Fig. 6(b).  $G_3$  is simplified and size-filtered to obtain an image  $G_4$ . LLM regions of the current lane in  $G_4$  are detected, in which the information on LLM in the previous image is also utilized. Fig. 6(c) shows  $G_4$  with the detected LLM and their fitted-lines, the two straight lines intersect at the point, i.e. QVP.  $G_3$  is also morphologically filtered to obtain  $G_5$  in Fig. 6(d). Using the detected LLM in the current input image, the ULM in the current input image is extracted in  $G_5$ . The lane detection algorithm that extracts lane markings separately according to pixels' positions is able to perform lane detection well.

Fig. 6(e) is 3D reconstruction from Fig. 6(d), in which black thick line and gray thin line express lane markings and fitted-lines of LLM, respectively. Two fitted-lines of LLM are almost parallel, which implies that the real inclination camera angle  $\theta$  is identical to the initial inclination camera angle  $\theta_0$ , and no modification of  $\theta$  is necessary. Lane parameters are estimated, and the vehicle deviation angle  $\gamma$  is  $-0.33^\circ$ , which indicates that the lane tangent bends to the left along the road. The lane width is about 3.57m. Radius of the lane curvature is 1044.32m. Fig. 6(f) shows the estimated lateral offsets  $x_0(y)$ , where the horizontal and vertical axes denote the distance from the vehicle and the corresponding lateral offset, respectively.  $x_0(y) > 0$  implies that the vehicle

locates at the right side of the lane center. For example, the lateral offset at 28m ahead of the vehicle is  $-0.245$ m. Figs. 6(g)-(j) show the result of obstacle detection, using BROT with a vertical line structuring element.

Fig. 7 show an example of lane detection from an input image with sloped road surface. Figs. 7(a) and (b) are a road image with an up-slope and its detected lane. Fig. 7(c) is 3D reconstructed images with  $\theta_0$  from Fig. 7(b). It is obvious that the two fitted-lines of LLM are not parallel, which is used to estimate  $\Delta\theta$ , and  $\Delta\theta$  is computed as  $0.4662^\circ$ . The reconstruction of Fig. 7 (b) with  $\theta_c (= \theta_0 + \Delta\theta)$  is shown in Fig. 7(d), in which more accurate lane parameters can be extracted.

To analyze performances of the proposed method in road image sequences, some results are shown in Fig. 8. Fig. 8(a) gives the slopes of the left and right LLM in the image sequence and their multiplication, where the horizontal axis expresses the frame number of the image sequence.  $\rho_R$  and  $\rho_L$  denote the slopes of the left and right LLM. When  $\rho_L$  increases, the absolute value of  $\rho_R$  decreases. The multiplication  $\rho_R \rho_L$  between  $\rho_R$  and  $\rho_L$  is approximate to a constant, and its mean and deviation are computed as  $-0.3687$  and  $0.0177$ , respectively. Variation of  $\rho_R \rho_L$  in Fig. 8(a) is mainly decided by three factors; that is, the slope of road surface, vehicle vibration, and the variation of lane width. Fig. 8(b) and (c) are the vehicle deviation angle  $\gamma$  and  $\Delta\theta$ , respectively. Fig. 8(d) is the estimated lateral offsets  $x_0(y_0)$  of the vehicle, here  $y_0 = 28$ m. Obviously, one main purpose of the driver assistant system is to keep the lateral offset of the vehicle in the right lane to be zero.

Fig. 9(a) is an image with white sign and characters on road surface, which results in some difficulties of lane detection in a single image. Based on the detected lane of the previous frame, Fig. 9(b) shows a good result of lane detection.

#### 5. Conclusions

A new method of detecting lane marking has been proposed for lateral control of a vehicle. The proposed method detects lane markings in a road image with two stages, first LLM and then ULM, based on their properties in 2D image plane and 3D road surface. Lane tracking is adopted to determine the location of the lane markings in sequence of consecutive images, using information about the lane location in previous images in the sequence to constrain the probable lane location in the current image. Geometric relations of lane structure between 2D image plane and 3D road surface are analyzed and employed to recalibrate camera. Additionally, an algorithm for obstacle detection is given based BROT, and used to control the longitude distance of the vehicle. The extracted lane structure parameters are used to analyze the vehicle heading direction, and control lateral and longitude distances of the vehicle.

#### References

- [1] E. D. Dickmanns, "Computer vision and highway automation," *Vehicle System Dynamics*, vol.31, no.5, p 325-344, 1999
- [2] J. C. Hsu, M. Tomizuka, "Analyses of vision-based

lateral control for automated highway system," *Vehicle System Dynamics*, vol.30, no.5, p.345-73, Nov. 1998

[3] J. D. Crisman and C. E. Thorpe, "SCARF: A Color Vision System That Tracks Roads and Intersections," *IEEE Trans. on Robot. Automat.*, vol.9, p.49-58, 1993

[4] M. Bertozzi and A. Broggi, "GOLD: a parallel real-time stereo vision system for generic obstacle and lane detection," *IEEE Trans. on IP*, vol.7, p.62-81, 1998

[5] D. Koller, Q. Luong, J. Malik, "Binocular stereopsis and lane marker flow for vehicle navigation: lateral and longitudinal control," Technical report UCB/CSD-94-804, March 1994

[6] H. Fritz, "Autonomous lateral road vehicle guidance using neural network controllers," Proc. of 3rd European Control Conference, ECC 95, vol.3, p.2748-53, 1995

[7] Sadayuki Tsugawa, Hiroaki Mori, Shin Kato, "A Lateral Control Algorithm for Vision-Based Vehicles with a Moving Target in the Field of View," IEEE Int. Conf. on Intelligent Vehicles, p.41-45, Oct., 1998

[8] D. Gualino, M. Parent, M. Uchanski, "Autonomous Lateral Control of a Vehicle Using a Linear CCD Camera," IEEE Int. Conf. on Intelligent Vehicles, 1998

[9] G. Y. Jiang, H. J. Kim, T. Y. Choi, "Indicatory sign recognition using a new morphological shape matching algorithm," *Journal of Electrical Engineering and Information Science*, vol.1, no.3, p.55-59, 1996

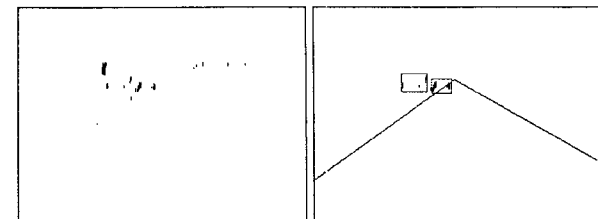
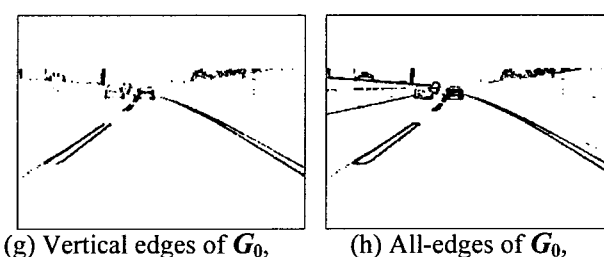
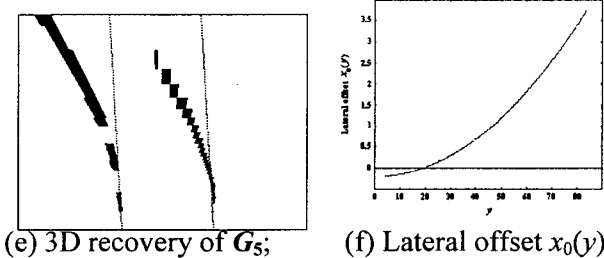
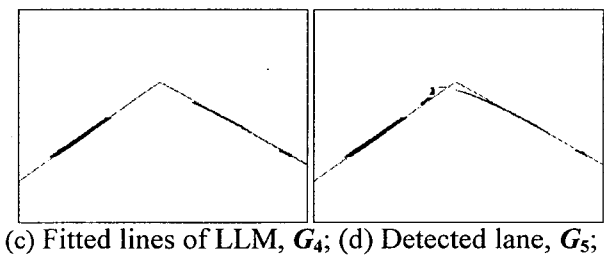
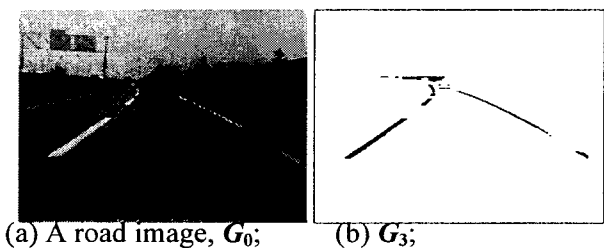


Fig. 6 One example of the tests

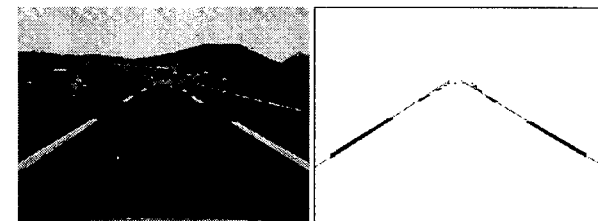


Fig. 4-35 A road image with up-sloped road surface

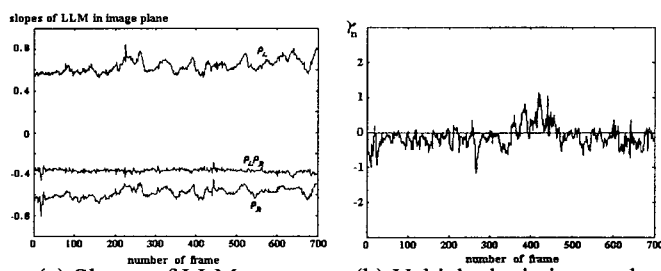


Fig. 8 Performance in a road image sequence

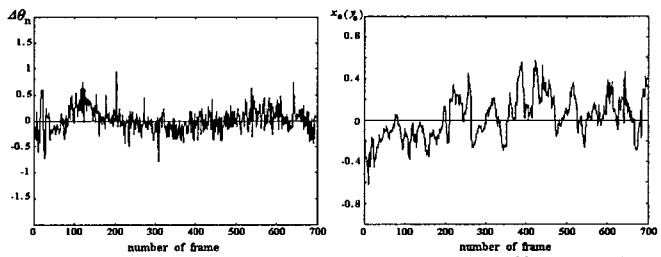


Fig. 8 Performance in a road image sequence

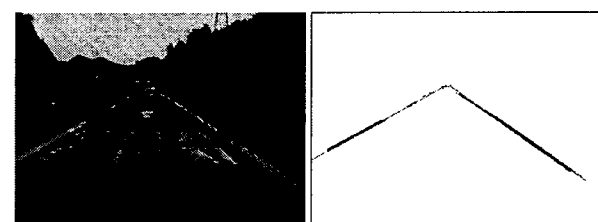


Fig. 9 Lane detection with lane tracking